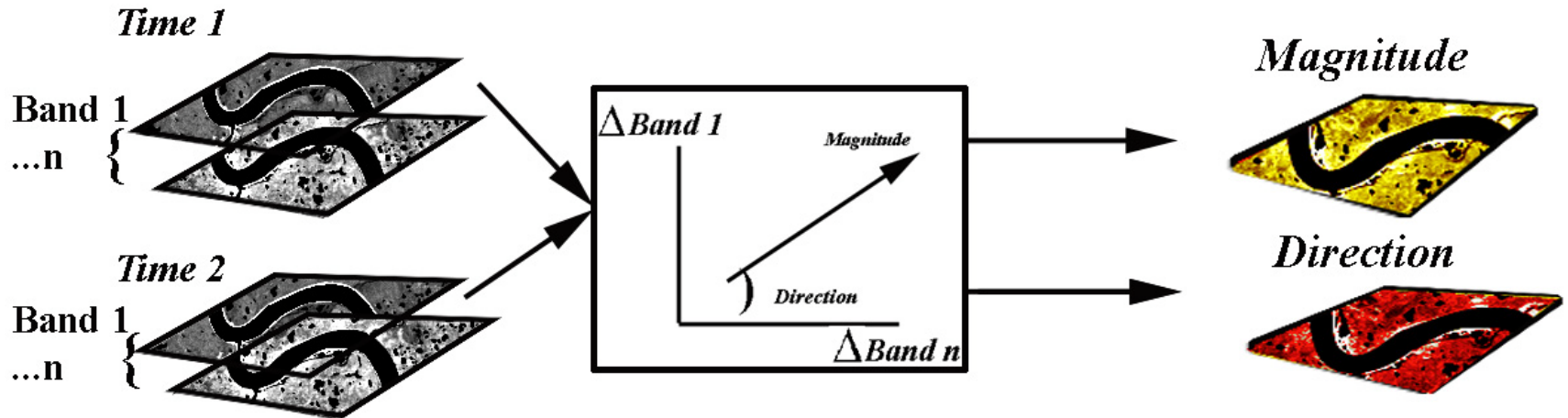


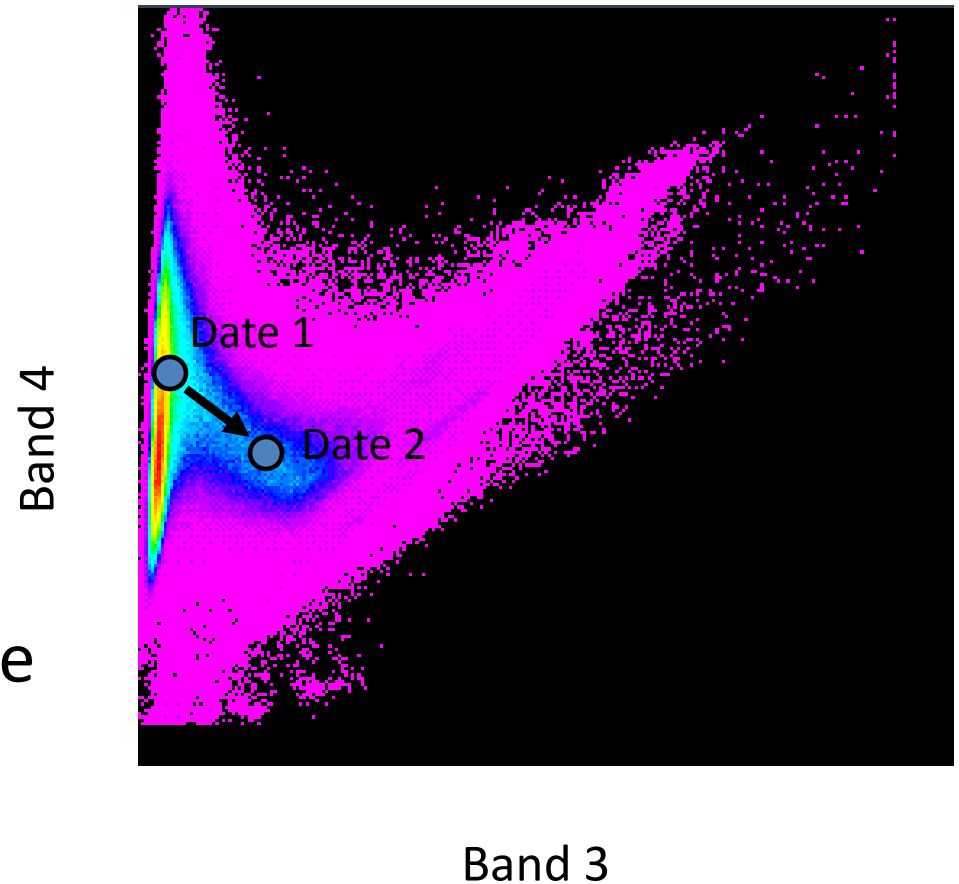
Change Vector Analysis (CVA)

Change Vector Analysis (CVA) uses two spectral channels to map both the: 1) magnitude of change and, 2) the direction of change between the two (spectral) input images for each date.



Change Detection: Methods

- Change vector analysis
 - In n-dimensional spectral space, determine length and direction of vector between Date 1 and Date 2



Change Detection: CVA

- No-change = 0 length
- Change direction may be interpretable
- Pick a threshold for change

Change Vector Analysis

Band Math followed by change vector

2-D change vector

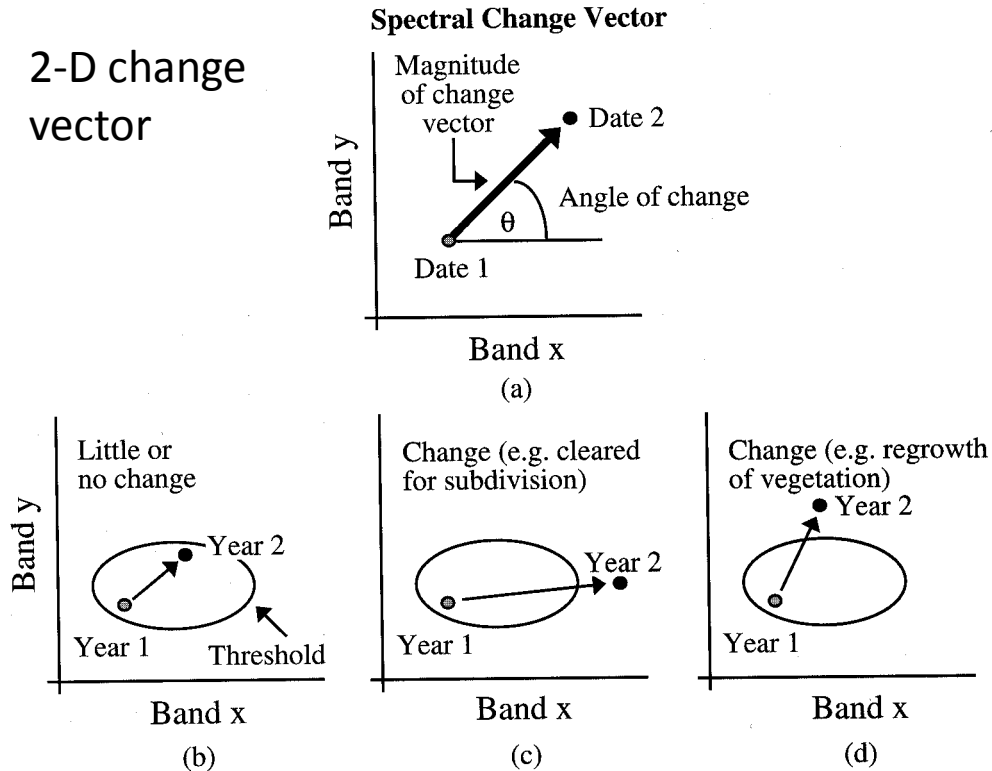


Figure 9-22 Schematic diagram of the spectral change detection method (after Malila, 1980).

3-D change vector

Possible Change Sector Code Locations for A Pixel Measured in Three Bands on Two Dates

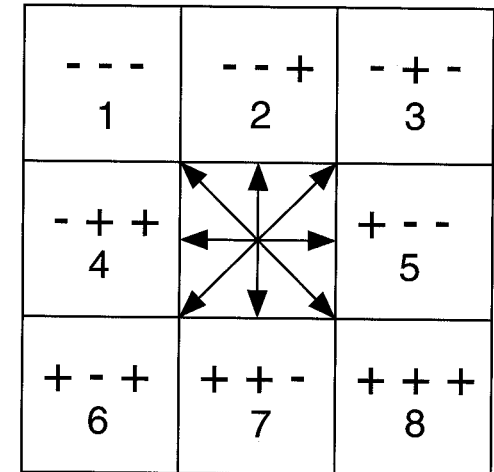


Figure 9-23 Possible change sector codes for a pixel measured in three bands on two dates.

Change Magnitude

Two dates, four bands

$$CM = \sqrt{(DN_{11} - DN_{21})^2 + (DN_{12} - DN_{22})^2 + (DN_{13} - DN_{23})^2 + (DN_{14} - DN_{24})^2}$$

where DN_{ij} is the digital number recorded in band j for date i .

Change Directions

Two dates, two bands

	-	Red	+
-	1	2	
NIR II	3	4	
+			

where

If $(DN_{22}-DN_{12}) < 0$ and $(DN_{24}-DN_{14}) < 0$ then direction = 1

If $(DN_{22}-DN_{12}) > 0$ and $(DN_{24}-DN_{14}) < 0$ then direction = 2

If $(DN_{22}-DN_{12}) < 0$ and $(DN_{24}-DN_{14}) > 0$ then direction = 3

If $(DN_{22}-DN_{12}) > 0$ and $(DN_{24}-DN_{14}) > 0$ then direction = 4

Two dates, three bands

Change Detection			
Sector Code	Band 1	Band 2	Band 3
1	-	-	-
2	-	-	+
3	-	+	-
4	-	+	+
5	+	-	-
6	+	-	+
7	+	+	-
8	+	+	+

A CHANGE VECTOR ANALYSIS TECHNIQUE TO MONITOR LAND USE/LAND COVER IN SW BRAZILIAN AMAZON: ACRE STATE

Rodrigo Borrego Lorena¹
João Roberto dos Santos¹
Yosio Edemir Shimabukuro¹
Irving Foster Brown²
Hermann Johann Heinrich Kux¹

¹ National Institute for Space Research - INPE
Av dos Astronautas, 1758 CEP 12.245-970 São José dos Campos – SP – Brazil
{rodrigo, jroberto, yosio, herman}@ltid.inpe.br
² UFAC - Universidade Federal do Acre – fbrown@mdnet.com.br

Abstract

The Brazilian Amazon is an area where extensive tropical rainforest areas are being destined to agriculture and cattle raising activities, contributing to the environmental and landscape change of this large region. In this context, the main objective of this paper is to present and test a technique for change detection called Change Vector Analysis (CVA) to analyze the variability of land use/land cover dynamics in the region of Peixoto, Acre State, using multitemporal analysis of multispectral TM-Landsat data. The results demonstrate the capacity of the CVA technique to stratify different types of change related to land use/land cover dynamics in this region.

- EXAMPLE CVA: The first step of the example CVA method was to apply a Tasseled Cap transform which generates the components Greenness and Brightness, in order to reduce the amount of redundant information of orbital images to be analyzed. This transform can be understood as defining a new coordinate system, where data from different bands occupy a new system of coordinates, where data from the different bands occupy new axes associated with biophysical properties of targets. In this case, such axes are Greenness, associated with the amount and vigor of vegetation, and Brightness, associated with variations of soil reflectance.
- The position variation of the same pixel during different data-takes within the space formed by these two axes, determines the magnitude and direction of the spectral change vectors.
- The next step in the band transformation process into new coordinates axes was to calculate the magnitude of variation among spectral change vectors between the images pairs.
- The magnitude of vectors was calculated from the Euclidean Distance between the difference in positions of the same pixel from different data-takes within the space generated by the axes Greenness and Brightness, as follows:

$$R = \sqrt{(yb - ya)^2 + (xb - xa)^2}$$

Where: R = Euclidean Distance

ya = DN values of Greenness from date 2

yb = DN values of Greenness from date 1

xa = DN values of Brightness from date 1

xb = DN values of Brightness from date 2

The angle of the vectors, which indicates the type of change that occurred, varies according to the number of components used (Table 1). In other words, each vector is a function of the combination of positive or negative changes through channels or spectral bands, which allows to distinguishing 2^{a} types of changes. Since only components Greenness and Brightness were used in this study, only four classes of change were possible.

Class	Brightness	Greenness	Themes
	-	+	Regrowth
	+	-	Deforestation
	+	+	Biomass Loss
	-	-	Burning or Water

Table 1 – Possible change classes from both input components and related types of change.

Class 1, which indicates increase in Greenness and decrease in Brightness, represents a direction of the vector that is mainly related to the growth of vegetation biomass, while Class 2, indicating decrease in Greenness and increase in Brightness, is strongly related to great losses of vegetation biomass as a result of the clear-cut of tropical forest. Class 3, indicating increase in Greenness and Brightness, is mainly related to smaller losses of biomass, such as transformation of sections with regrowth or cultures, as large as bushes, to pasture. Examples of change classes are shown in Figure 3.

A threshold of final magnitude was defined for each one of the change classes through an interactive adjustment (Table 2). The final result of the CVA technique is an image of vector change, where the main function of the threshold was to filter out the valueless spectral information, preserving just those information that are related to each of the Classes of Change.

Classes of Change	Thresholds 1990/1997	Thresholds 1997/1999
 Class 1	10	10
 Class 2	20	17
 Class 3	22	7
 Class4	40	40

Table 2 - Magnitude thresholds of change for each class during each data-take analyzed.

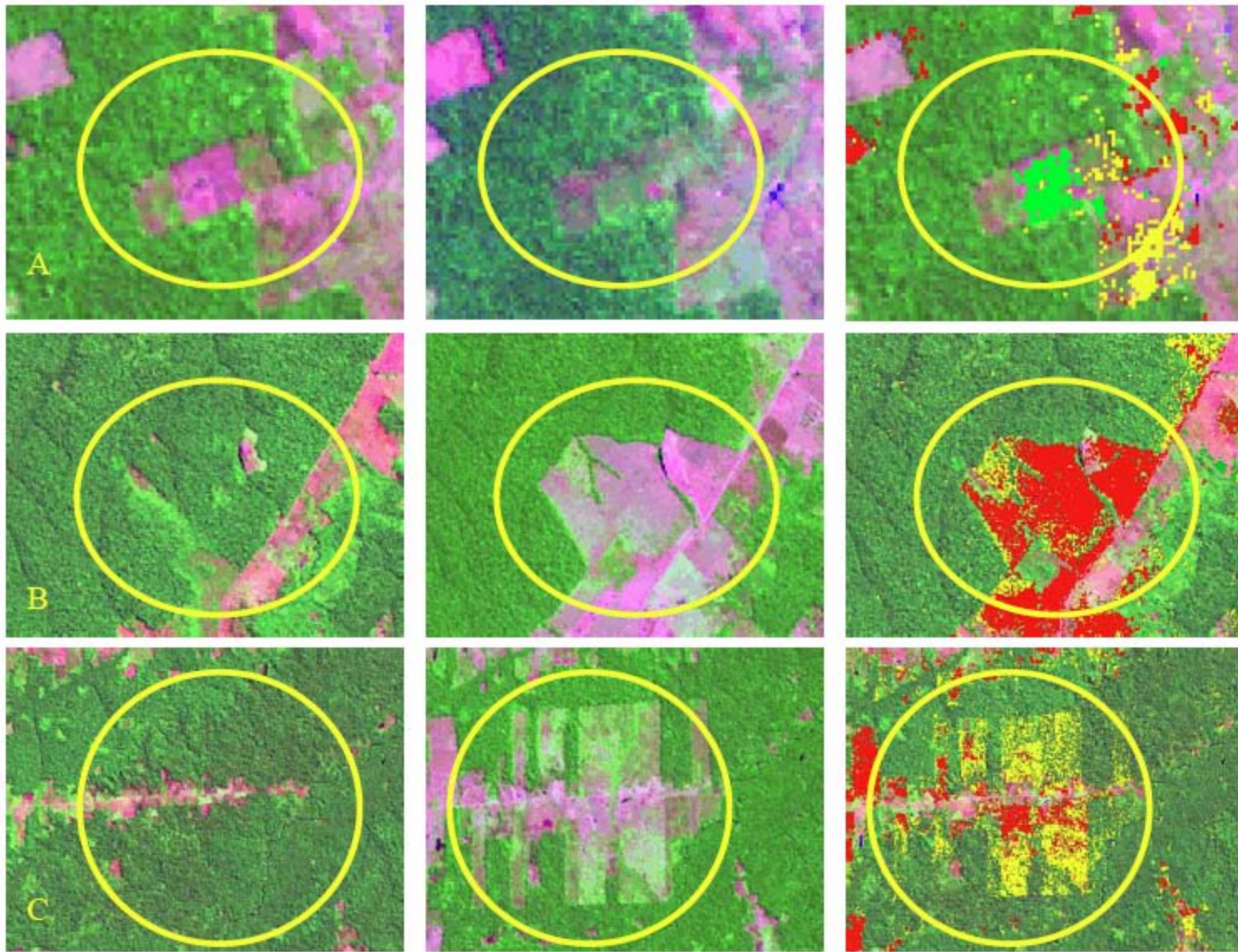


Figure 3 – Examples of thematic changes: (A) Class of change 1 = biomass growth; (B) Class of change 2 = deforestation; (C) Class of change 3 = low biomass loss.

- The final product generated using this technique, namely a mask related to 4 possible Classes of Change, was obtained by crossing a grid containing the magnitude values of Vector Changes with the four possible Classes of Change, following the threshold procedure previously described.
- It was further defined that Class 1, which represents biomass growth, would be represented by green; Class 2, that represents deforestation, by red; Class 3, that represents, among other things, biomass loss derived not from primary forest to bare soil or pasture (lower biomass loss), would be represented by yellow. Class 4, which refers either to the increase in water body coverage area or to areas burned during the second data-take, would be represented by blue.

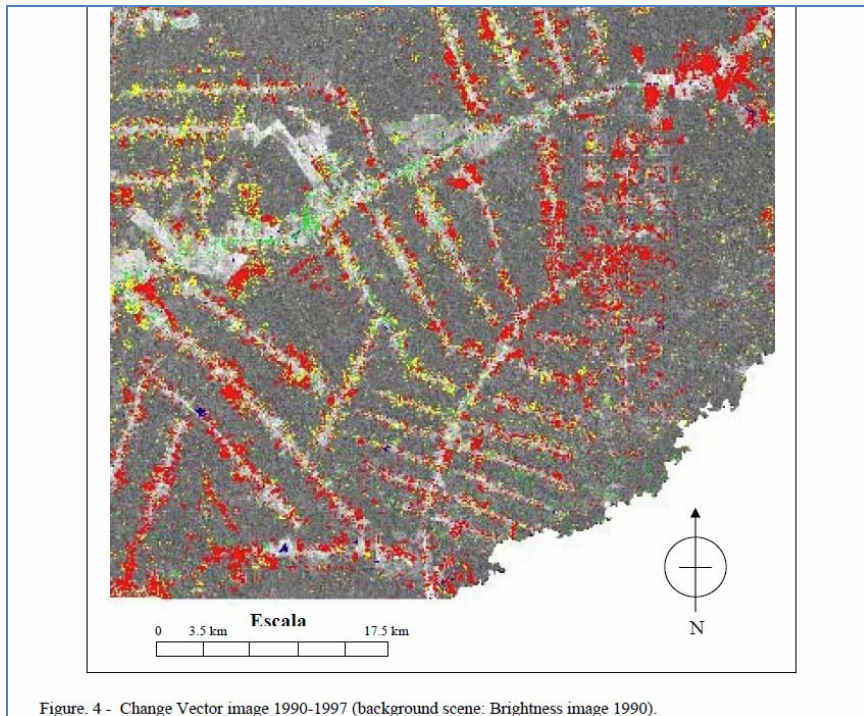


Figure. 4 - Change Vector image 1990-1997 (background scene: Brightness image 1990).

- The results obtained by the application of the Change Vector Analysis technique demonstrate the capacity to detect and stratify different types of changes in terms of biomass gain and loss. The Change Vector image of the two periods studied allowed to verify that the deforested area was 850 Km² in the 1990-99 period.
- The annual rate deforestation is 86 Km² /year for the period between 1990 and 1997, increasing to 165 Km² /year between 1997 to 1999. In future studies we intend to test the components from other types of linear transformations, such as those components derived from processes such as Spectral Mixture Linear Model and Principal Components.
- Taking into account that the CVA procedures were derived from the Tasseled Cap analysis (Greenness and Brightness components), in temperate and sub-tropical regions, these techniques must be further analyzed and adapted to be used in tropical regions.
- Changes introduced in the the study area by human activity and their relationship with primary and secondary vegetation were evaluated by the information obtained from field survey about present and past land use/land cover characteristics. These data were saved on a database that along with the results obtained from satellite data analysis could facilitate the understanding of the changes that took place in the landscape.

Using remote sensing to assess tsunami-induced impacts on coastal forest ecosystems at the Andaman Sea coast of Thailand

H. Roemer¹, G. Kaiser¹, H. Sterr¹, and R. Ludwig²

¹Department of Geography, Christian-Albrechts-Universität zu Kiel, Kiel, Germany

²Department of Geography, Ludwig-Maximilians-Universität München, Munich, Germany

Received: 22 December 2009 – Revised: 16 March 2010 – Accepted: 20 March 2010 – Published: 13 April 2010

- The December 2004 tsunami strongly impacted coastal ecosystems along the Andaman Sea coast of Thailand.
- In this paper tsunami-induced damage of five different coastal forest ecosystems at the Phang-Nga province coast is analyzed with a remote sensing driven approach based on multi-date IKONOS imagery.
- Two change detection algorithms, change vector analysis (CVA) and direct multi-date classification (DMC), are applied and compared regarding their applicability to assess tsunami impacts.

4.1 Pre-processing

Before applying change detection analyses, the digital numbers from IKONOS imagery (DN_λ) were converted into at sensor's aperture radiance values (L_λ), according to the equation (Taylor, 2009):

$$L_\lambda = \frac{10^4 \cdot DN_\lambda}{\text{CalCoef}_\lambda \cdot \text{Bandwidth}_\lambda},$$

where,

DN_λ = digital value for spectral band λ ,

CalCoef_λ = Radiometric calibration coefficient
($\text{DN}/(\text{mW}/\text{cm}^2\text{-sr})$)

Bandwidth_λ = Bandwidth of spectral band λ (nm).

Both CalCoef_λ and Bandwidth_λ are given in Table 1.

Table 1. IKONOS band dependent parameters of the scenes acquired on 13 January 2003, 04:11 GMT (pre-tsunami) and 15 January 2005 04:12 GMT (post-tsunami), after Taylor (2009), Geoeye (2006).

IKONOS band (λ)	spectral range (nm)	band-width (nm)	resolution (m) nadir/26° off nadir	CalCoef_λ^* ($\text{DN}/(\text{mW}/\text{cm}^2\text{-sr})$)
Pan	526–929	403	0.82/1.0	161
Blue	445–516	71.3	3.2/4.0	728
Green	506–595	88.6	3.2/4.0	727
Red	632–698	65.8	3.2/4.0	949
NIR	757–853	95.4	3.2/4.0	843

* Only for image production date Post 22 February 2001 (coefficients are for the 11-bit products).

Geometric correction (co-registration) was carried out by using a set of ground control points from the pre-tsunami scene. The post-tsunami scene was then warped to the base image. The dark object subtraction, one of the simplest and most widely used image-based absolute atmospheric correction approaches, was applied for radiometric correction (Spanner et al., 1990; Ekstrand, 1994).

Image pan-sharpening was applied using the Gram-Schmidt Spectral Sharpening approach (Laben and Brower, 2000). Therewith, the low resolution multispectral data (4 m) were sharpened using the high spatial resolution panchromatic band (1 m). The resulting high-resolution multispectral dataset (Fig. 3) was used to visually select training areas and for identifying appropriate test sites for the accuracy assessment of change classifications.

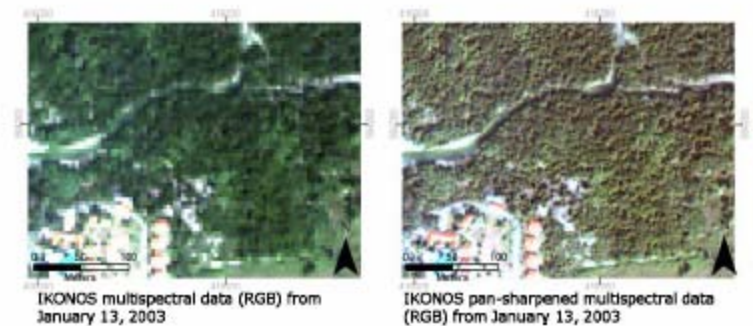


Fig. 3. IKONOS pan-sharpening based on the Gram-Schmidt-spectral sharpening technique (northern Khao Lak).

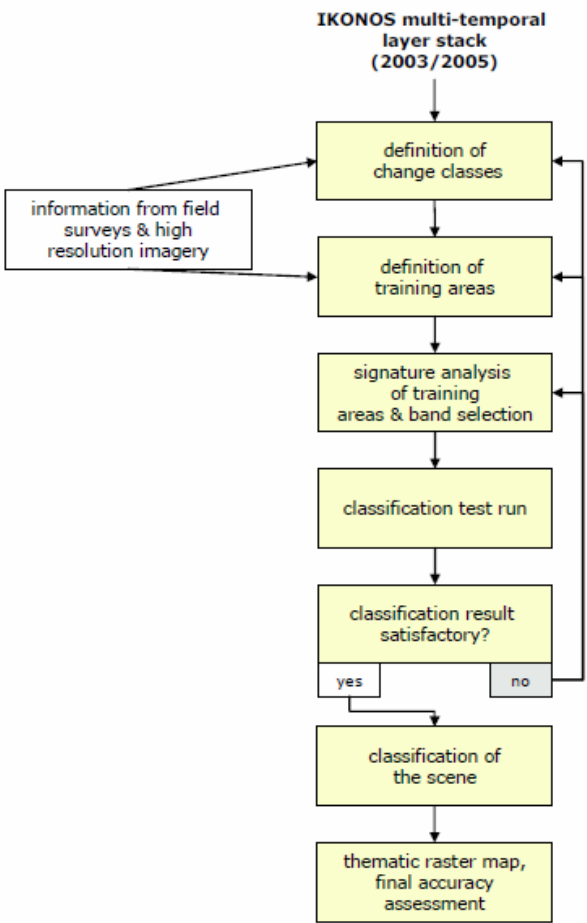


Fig. 4. Flowchart of direct multi-date supervised classification.

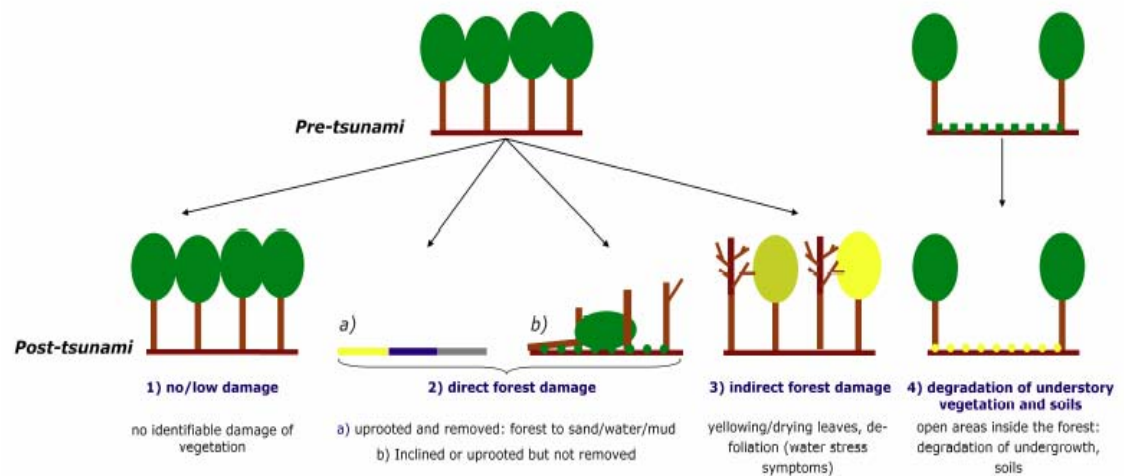
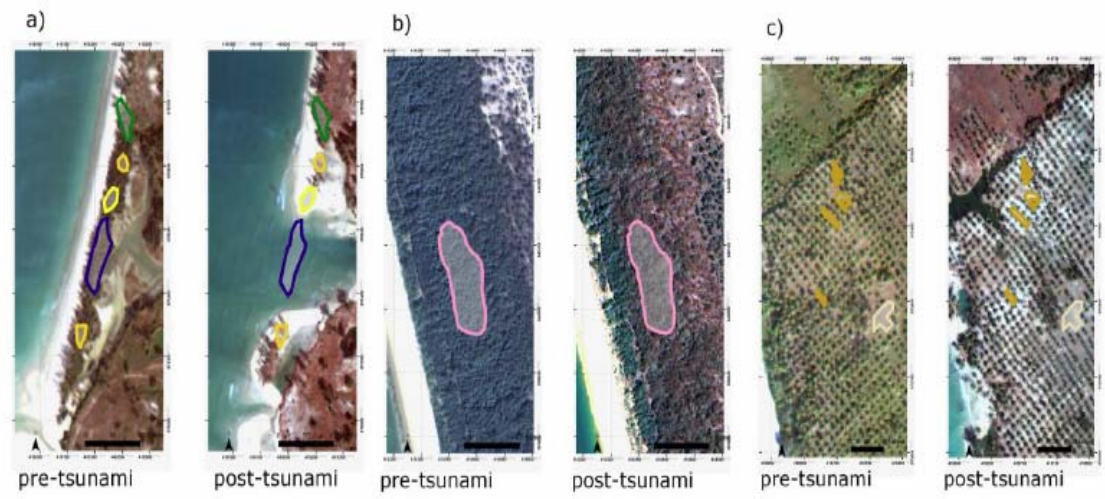


Fig. 5. Categorization of forest damage patterns.



- direct forest damage: forest to water
- direct forest damage: forest to sand
- direct forest damage: uprooted; roots/trunks remaining
- no damage of vegetation
- indirect forest damage: yellowing / defoliation
- degradation of soils/understory (understory to bare soil)
- degradation of soils/understory (understory to sand)

- A first step of CVA involves the calculation of the tasseled cap components brightness (TC 1) and greenness (TC 2), in order to reduce the amount of redundant information of digital images to be analyzed (Kauth and Thomas, 1976). This process can be compared to defining a new two-dimensional feature space, in which the multispectral data occupy two new axis associated with biophysical properties in the areas of interest.

- According to Lorena et al. (2002), the brightness axis is correlated to variations of soil reflectance whereas the greenness axis is associated with amount and vitality of vegetation.

- Tasseled cap components were calculated for IKONOS multispectral data according to the equations (Horne, 2003):

$$TC\ 1=0.326\cdot x_{blue}+0.509\cdot x_{green}+0.560\cdot x_{red}+0.567\cdot x_{nir}$$

$$TC\ 2=-0.311\cdot x_{blue}-0.356\cdot x_{green}-0.325\cdot x_{red}+0.819\cdot x_{nir}$$

The direction or angle of the change vector is determined by the type of occurring change. Due to the fact that only two components are used for CVA, only four major change directions are possible:

- **0–90: increase in both components,**
- **90–180: increase in brightness, decrease in greenness,**
- **180–270: decrease in both components,**
- **270–360: decrease in brightness and increase in greenness.**

- Similar to a decision tree classification, the final definition of change classes (Table 4) was carried out by user defined thresholds of direction and magnitude values. Spectral statistics of training areas, computed for the multi-date Classification, were used for decision support.
- The threshold distinguishing between change- and no-change-information (31.49) was defined based on the first standard deviation from the mean magnitude calculated for training class IDs 1 and 2 . Another threshold of 46.06 was defined based on 1.5 times the standard deviation of the vector's magnitude.

Table 4. Change class definition based on CVA.

change classes (ID/name)	aggregated change classes	direction (°)/ magnitude	test area n*
1 no damage	no damage	-/≤31.49	988
2 regrowth		0-90/>31.49	
3 other	other	270-360/>31.49	-
4 sand → water	understory/soils to water	250-270/>31.49	150
5 mud → water		225-250/31.49-46.06	
6 understory → water		225-250/>46.06	
7 forest → water	direct forest damage (forest to water/mud)	180-225/>46.06	187
8 forest → mud		180-225/31.49-46.06	143
9 degradation	degradation	90-180/>31.49	613

= number of pixels (total number of image pixels 5.04×10^5 pixels).

- The analysis shows that DMC outperforms CVA in terms of accuracy (Kappa values for DMC ranging between 0.947 and 0.950 and between 0.610–0.730 for CVA respectively) and the degree of detail of the created change classes.
- Results from DMC show that mangroves were the worst damaged among the five forests, with a 55% of directly damaged forest in the study area, followed by casuarina forest and coconut plantation.
- Although technical implementation of CVA is easier than DMC, both methods require producer's expertise in order to correctly interpret change detection results. Disadvantages in DMC involve the problem of considering many different types of change classes during the classification process and the fact that the degree of automation is relatively low.
- Performing CVA is quicker in the beginning phase, since rough change information can be automatically extracted from the change vector's magnitude and direction. The challenge here lies in the selection of appropriate change thresholds and further differentiations of change classes (interpretation). Thus, expenditure of time and work is almost the same for both methods with some advantages for CVA.

3 Sampling Scheme

3.1 Sample Design

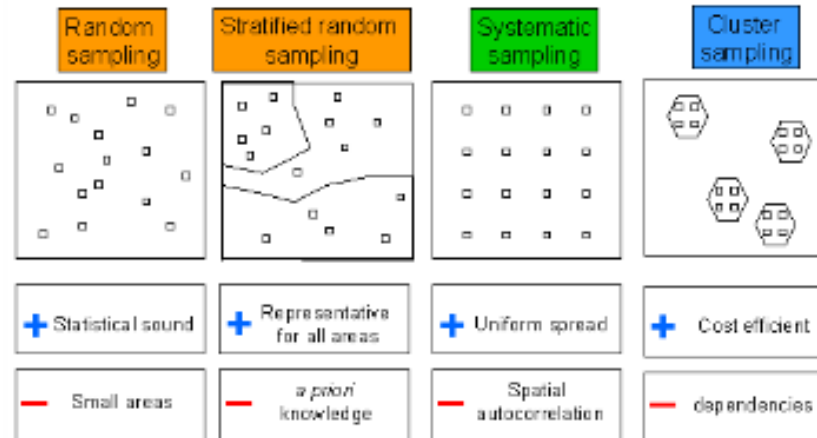
Assessing the accuracy of maps derived from remote sensing data is both time- and money-consuming. Due to the fact that it is not possible to check whole mapped areas, sampling becomes the means by which the accuracy of land-cover maps can be derived (Congalton, 1988a). As stated by Ginevan (1979) any sampling scheme should satisfy three criteria:

1. It should have a low probability of accepting a map of low accuracy.
2. It should have a high probability of accepting a map of high accuracy.
3. It should require a minimum number, N , of ground truth samples.

Therefore researchers have published formulas to calculate the numbers of sample plots which are dependent on the objectives of the project (van Genderen and Lock, 1977; Rosenfield, Fitzpatrick-Lins and Ling 1982; Rosenfield, 1982; Congalton, 1991). These formulas are discussed in 3.3. The sampling schemes that have been used are:

- Simple Random Sampling (SRS).
- Stratified Random Sampling (STRAT).

Figure 3: Sampling designs used for accuracy assessment and rough evaluation of the different approaches.



- Systematic Sampling (SYS).
- Stratified Systematic Unaligned Sampling (SSUS).
- Cluster Sampling (CLUSTER).

Figure 3 illustrates the various sampling approaches and lists their major advantages and drawbacks. The choice of sampling technique will depend upon several factors, including the size of the study area, the type and distribution of features being mapped, and the costs of acquiring verification data.

3.1.1 Random sampling

The simple random sampling (SRS) yields too many samples in larger areas and too few samples in smaller areas (Congalton, 1988a). As the SRS is area-weighted, it is generally accepted that some kind of stratified sampling should be used, thereby ensuring that each class is adequately tested (Aronoff, 1985). The definition of strata requires knowledge of the population that will be assessed; classification of the remotely sensed data must therefore be performed before field verification (Fenstermaker, 1991). This can lead, in some projects, to serious problems because of the temporal change of land-cover between the time of image acquisition and field verification (Congalton, 1991).

3.2 Systematic Sampling

In systematic sampling approaches, the sampling unit is selected at an equal interval over space. The advantage of systematic sampling is the convenience of obtaining

Table 1: Sample schemes discussed by different authors.

SRS ¹	STRAS ²	SYS ³	SSUS ⁴	CLUSTER ⁵
Congalton, 1988a Aronoff, 1985	Card, 1982 Hay, 1979 Ginevan, 1979 Congalton 1988a Fitzpatrick-Lius, 1981 Hord and Bronner, 1976 Van Genderen and Lock, 1977	Congalton, 1988a Warren <i>et al.</i> , 1990	Berry and Baker, 1968 Aronoff, 1985	Congalton 1998a Stehman, 1997 Janssen <i>et al.</i> , 1994

1 = simple random sampling, 2 = stratified random sampling, 3 = systematic sampling, 4 = stratified systematic unaligned sampling, 5 = cluster sampling.

the sample and the uniform spread of the sampled observations over the entire population (Cochran, 1977). An obvious problem in systematic sampled population is the bias that exists if the population shows some kind of spatial autocorrelation. If the presence, absence, or degree of certain characteristics affects those in neighboring units, then the phenomenon is said to exhibit spatial autocorrelation (Cliff and Ord, 1973). Work by Congalton (1988b) on Landsat MSS data from three areas of varying spatial diversity (agricultural land, range land, and a forest site) showed a positive influence, as much as 30 pixels. If spatial autocorrelation analysis indicates periodicity within the data, then the use of systematic sampling schemes may result in poor estimates of classification accuracy (Fenstermaker, 1991).

3.2.1 Stratified systematic unaligned sampling

A systematic sampling ensures that sample points of one class are sampled from the entire area (see *Figure 4*). This assumes that the class areas are randomly distributed over the area, but commonly most classes show some form of clumped distribution (e.g., urban areas), or regular distribution (e.g., regular road network) (Aronoff, 1985). If the distribution of the polygons tends toward a direction parallel to the transects of the systematic sampling, a significant bias can be introduced. An unaligned systematic sample can be used to eliminate this bias. As described by Berry and Baker (1986), a stratified systematic unaligned sampling combines the advantage of randomization and stratification with the useful aspects of systematic sampling, while avoiding the possibilities of bias due to the presence of periodicities.

3.2.2 Cluster sampling

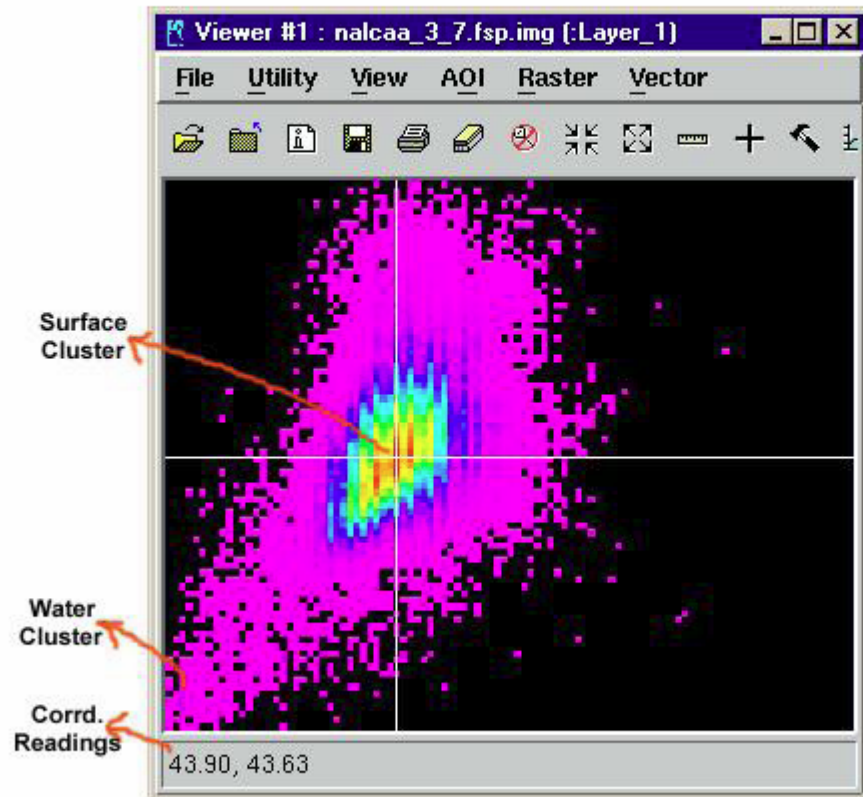
Cluster sampling is a technique of sampling in which units are not single pixels but groups of pixels. The idea is that it is much easier and cheaper to visit a few large areas than many small areas. Congalton (1988b) suggest that the rate of homogeneity, a coefficient of intraclass correlation, determines whether the chosen clusters are useful for accuracy assessment. The more heterogeneous the pixels within one cluster, the higher the intraclass coefficient; which is favorable when using cluster sampling. The size of the clusters should be smaller than 10 pixels and should never exceed 25 pixels.

3.2.3 Recommendations for the sampling design

Congalton (1991) suggested a combination of stratified and random sampling. The stratified sampling can be done in conjunction with training data collection in an early phase of the project. After the first classification results, stratified random sampling completes the data collection necessary for accuracy assessment. Fenstermaker (1991) proposes a multistage sample approach for large area sampling.

- Another technique is an automatic scattergram-controlled regression (ASCR) method, developed by Elvidge et al. (1995) for use with large sets of Landsat images.
- This method uses scattergrams of the near-infrared bands of image date 1 and date 2 to identify stable land and water data clusters and generate an initial regression line between the two cluster centers.
- A no-change pixel set is selected by placing thresholds about this line. These pixels are then used in the regression analysis of each band to derive gains and offsets for the radiometric normalization. Requirements for this method are that:
 1. Images are acquired under similar solar and phenological conditions.
 2. Land cover for a large portion of the image in the time covered by the images to be rectified has not changed.
 3. There are both land and water pixels in the scene.

- This method is shown to significantly reduce **haze**, making images more comparable spectrally. The researchers also list advantages of this procedure over other linear relative normalization methods:
 1. Cloud/shadow/snow effects are reduced compared with simple regression methods.
 2. A large percentage of the total number of image pixels is used.
 3. Normalization errors are distributed among different land cover types.
 4. The necessity of identifying bright and dark radiometric control pixels is eliminated.
 5. The speed of the normalization procedure is accelerated by reducing human intervention (though it may not reduce the computation time).



ASCR

1. Compute scattergrams of NIR bands
2. Identify water and land centers on both scattergrams, formulate no-change area definitions, and select pixels within no-change areas
3. Compute regression models for all bands using only pixels within no-change areas
 $Y = a X + b$
Y: reference image
X: image to be normalized
4. Normalize image using the regression models
 $X' = a X + b$
X': normalized image

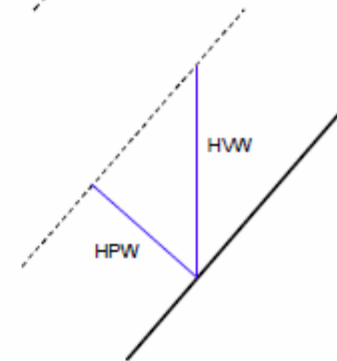
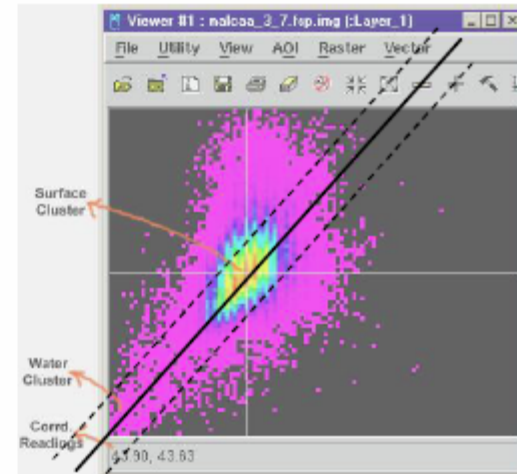
No-Change Areas

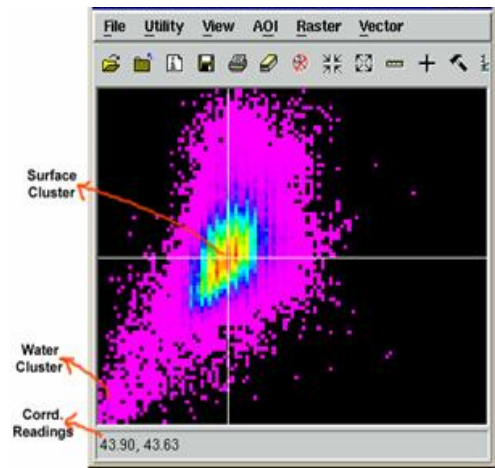
Known:

- x and y coord of land and water centers
- Half perpendicular width (HPW) ~ 10 DN

Find the area between the parallel dashed lines:

- Solid line $y = ax + b$
Slope $a = (y_2 - y_1) / (x_2 - x_1)$
Intercept $b = y_1 - ax_1$
- Half vertical width (HVV)
 $HVV = \text{SQRT}(1 + a^2) * \text{HPW}$
- Areas between dashed lines
 $|y - ax - b| \leq HVV$





Once you have the coordinates of these clusters, you then calculate a and b using the following equations:

$$a = \frac{j_{i_{max}} - j_{j_{max}}}{i_{i_{max}} - i_{j_{max}}} \quad b = j_{i_{max}} - a \times i_{i_{max}}$$

Write down the values in the table below.

	$i_{i_{max}}, j_{i_{max}}$	$i_{j_{max}}, j_{j_{max}}$	a	b
Band 3-7 pair (NIR1)				
Band 4-8 pair (NIR2)				

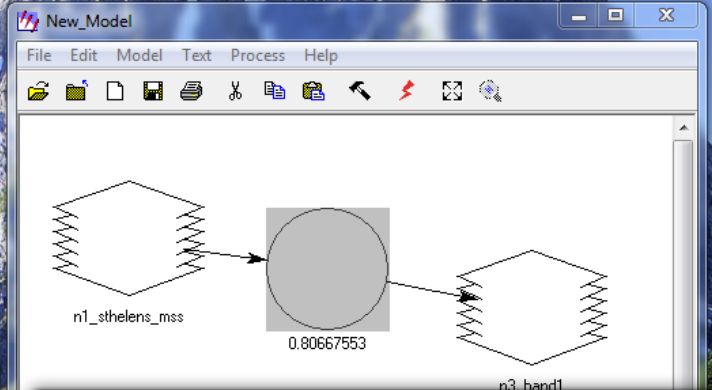
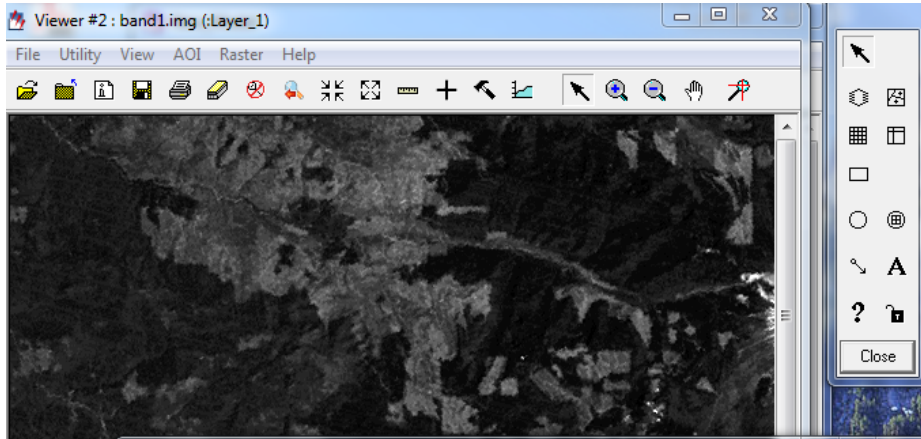
a and b are used to estimate the half vertical width (HVW_{NC}) of no-change area from half perpendicular width (HPW_{NC}). We will use an HPW_{NC} value of 4 DN in this exercise. HVW_{NC} and HPW_{NC} have the following relationship:

$$HVW_{NC} = \sqrt{1+a^2} \times HPW_{NC} = \sqrt{1+a^2} \times 4$$

You will calculate HVW_{NC3} and HVW_{NC4} for band 3 and 4 scatterplots using the “a” values of band 3 and 4. Based on experience, the values for HVW_{NC} shouldn't be too large. The reasonable range is between 10 and 13 DN. Write down your HVW_{NC3} and HVW_{NC4} values below.

HVW _{NC3}	
HVW _{NC4}	

iumax	jumax	imax	jmax		
28.05	34.92	5.03	7.98		
	26.94	jumax-jmax	top	5.886542137	a*imax
	23.02	iumax-imax	bottom	2.093457863	jmax-a*imax
	1.170287	top/bottom		2.09346	b
	1.17029	a			
1+a squard	2.36957				
squareroot	1.539341				
timrs 4	6.157364				
HVWnc3	6.157364				



ImageInfo (band1.img)

File Edit View Help

Layer_1

General | Projection | Histogram | Pixel data

File Info:
 Layer Name: Layer_1 File Type: IMAGINE Image
 Last Modified: Tue Apr 27 05:25:07 2010 Number of Layers: 1
 Image/Auxiliary File(s): All File Size: 0.83 MB

Layer Info:
 Width: 917 Height: 772 Type: Continuous
 Block Width: 512 Block Height: 512 Data Type: Unsigned 8-bit
 Compression: Run-Length Encoding (ESRI) Data Order: Mixed
 Pyramid Layer Algorithm: IMAGINE 2X2 Resampling

Statistics Info:
 Min: 0 Max: 151 Mean: 16.528
 Median: 15 Mode: 13 Std. Dev: 8.546
 Skip Factor X: 1 Skip Factor Y: 1
 Last Modified: Tue Apr 27 05:25:55 2010

Map Info (Pixel Center):
 Upper Left X: 527364.0 Upper Left Y: 5124984.0
 Lower Right X: 579576.0 Lower Right Y: 5081037.0
 Pixel Size X: 57.0 Pixel Size Y: 57.0
 Unit: meters Geo. Model: Map Info

Function Definition: 0.80667553

File Edit Model Text Process Help

Available Inputs:

- \$n1_sthelens_mss
- \$n1_sthelens_mss(1)
- \$n1_sthelens_mss(2)
- \$n1_sthelens_mss(3)
- \$n1_sthelens_mss(4)
- \$n1_sthelens_mss(5)
- \$n1_sthelens_mss(6)
- \$n1_sthelens_mss(7)
- \$n1_sthelens_mss(8)

Functions: Analysis

- CLUMP (<layer> , 4)
- CLUMP (<layer> , 8)
- CONVOLVE (<raster> , <kernel>)
- CORRELATION (<covariance_matrix>)
- CORRELATION (<raster>)
- CORRELATION (<raster> , IGNORE <covariance_matrix>)
- COVARIANCE (<raster> , IGNORE <covariance_matrix>)
- DELRDWS (<dsctable> , <sievetable>)
- DIRECT LOOKUP (<arg1> , <table>)
- EIGENMATRIX (<matrix1>)
- EIGENVALUES (<matrix1>)

0.80667553 * \$n1_sthelens_mss(1) + -0.05273760

OK Clear Cancel Help